JET-P(94)62

The JET Programme I & II

D J Campbell

JET Joint Undertaking, Abingdon, Oxfordshire, OX14 3EA, UK.

Preprint of a paper to be submitted for publication in the Proceedings of
36eme Cours de Perfectionnement de AVCP, (March 1994)

November 1994

The JET Programme I:

Magnetohydrodynamic Stability, Confinement and Current Drive

D J Campbell
JET Joint Undertaking, Abingdon, Oxon, OX14 3EA, UK

Abstract

The major results from experiments performed in the Joint European Torus are reviewed. Extensive investigations of mhd stability properties of the plasma have been conducted and the regions of stable operation are now well understood, though much basic physics remains unresolved. Confinement studies have been undertaken in both L- and H-mode regimes and the scaling of energy confinement with major plasma parameters has been identified. Current drive studies have addressed both the problem of global current drive, either by lower hybrid wave drive or by bootstrap current, and that of local current profile control for the stabilization of mhd instabilities. The discussion necessarily concentrates on the broad themes of the programme rather than the details of the underlying physics.

1. Introduction

The Joint European Torus is a joint undertaking by 14 European states operating under the auspices of EURATOM. The essential objective of the experiment is to study plasmas in conditions and dimensions approaching those needed in a thermonuclear reactor. This involves four main areas of work [1]:

- The scaling of plasma behaviour as parameters approach the reactor range;
- The investigation of plasma-wall interactions in these conditions;
- The study of plasma heating in reactor relevant conditions;
- The study of α-particle production, confinement and consequent plasma heating.

In the last 11 years, experiments have concentrated on studies of plasma heating, confinement and mhd stability at temperatures and densities approaching those required for a reactor. Attention is now shifting to the investigation of plasma-wall interactions and a new phase of

the JET programme has just begun which will concentrate on this question. This new phase is discussed in the second lecture on JET. Although initial experiments with a deuterium-tritium mixture were carried out in 1991, these were of a preliminary nature and a full study of DT plasmas and α-particle relevant issues is not anticipated before 1996.

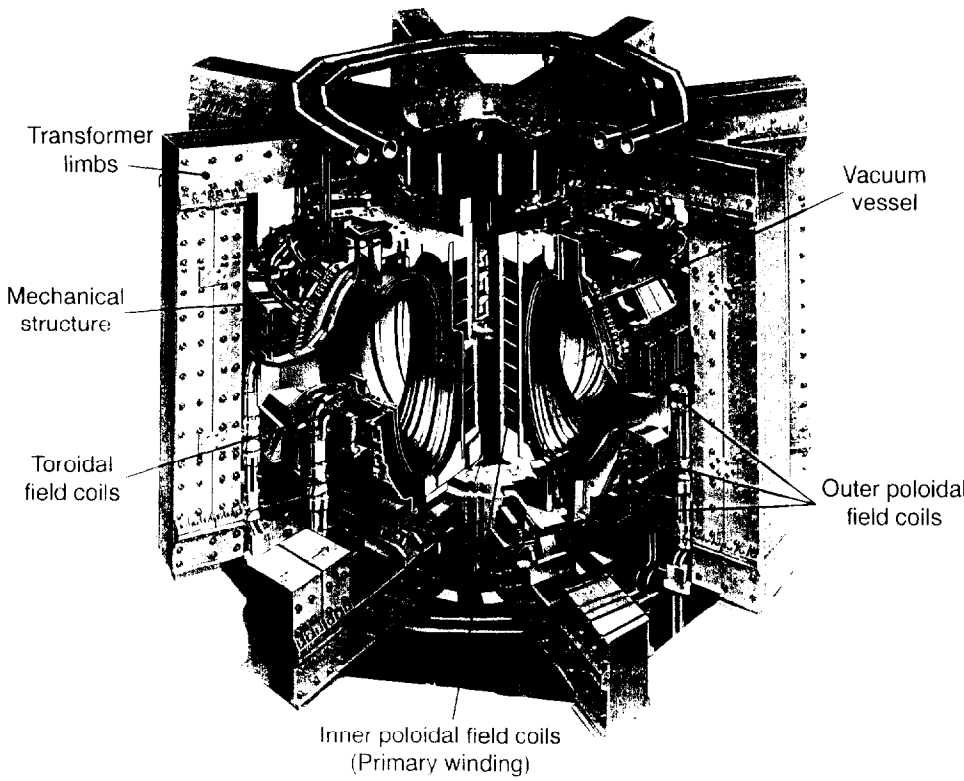

Fig. 1: Overview of the JET tokamak

2. The JET Tokamak

Construction of JET (Fig. 1) began in 1978 and the design of the tokamak reflects several aspects of our understanding of tokamak physics at that time. In particular, JET was designed as a limiter device, though subsequent developments allowed operations with an internal magnetic separatrix and access to the H-mode. There were, in addition, novel aspects of the design such as the elongated cross-section, which was devised to minimize the stresses in the toroidal field (TF) coils. This has provided JET with the flexibility to adapt to the changing demands of fusion research and to remain at the forefront of the magnetic fusion programme. The principal parameters of the JET tokamak are given in Table 1.

The JET heating systems have been designed for high power, long pulse operation. In the most recent experimental campaign, neutral beam injection (NBI) provided 18MW of injected power for up to 10s at injection energies of up to 150keV in deuterium, tritium, or helium-3 according to the experimental requirements. The ion cyclotron radio frequency (ICRF) system

had an installed generator capacity of 32MW for 20s and operated over the range 23-57MHz so as to permit heating over a range of magnetic fields and minority resonance positions. In addition, the control system permitted operation of the antennas as a phased array for current drive studies. Current drive experiments principally exploited the lower hybrid current drive (LHCD) system, operating at 3.7GHz, which had a generator capacity of 4MW for 20s.

Table 1: Principal parameters of the JET tokamak

Parameter	Design value	Experimental values
Major radius, R (m)	3	2.5 - 3.4
Minor radius, a (horizontal)	1.25	0.8 - 1.2
Minor radius, b (vertical)	2.1	0.8 - 2.1
Toroidal magnetic field (at R=3m), B_φ (T)	≤ 3.45	≤ 3.45
Plasma current, I_p (MA): limiter	4.8	7.1
X-point	-	5.1

Considerable progress has been made in JET in the exploitation of high power ICRF heating [2], particularly in suppressing processes contributing to impurity generation, which previously limited the effectiveness of this heating method. The principal process giving rise to impurities appears to be sputtering from the antenna Faraday screen as a result of RF field rectification. By appropriate phasing of the current strips within the antennas, aligning of the Faraday screen with the magnetic field at the plasma edge and using beryllium in the fabrication of the Faraday screen, generation of impurities has been eliminated as a serious problem.

The flexibility of the JET experiment permits a wide range of plasma configurations to be used. Both limiter and internal magnetic separatrix (X-point) configurations have been investigated, the latter allowing access to the improved confinement of the H-mode. Fig. 2 illustrates equilibria at the highest currents in each of the most common plasma configurations. The plasma facing surfaces used in the most recent (1991-1992) experimental campaign are also indicated. Beryllium was introduced into JET in 1989, both as a limiter and a getter material [3]. It was found to be very effective in reducing oxygen concentrations in the plasma, but suffered from melting above 1270°C. As a result, graphite, often in the form of carbon fibre composites, which have high thermal conductivity and resistance to thermal stresses, was retained for certain plasma facing surfaces to permit operation at low to moderate densities where the optimum fusion performance is obtained.

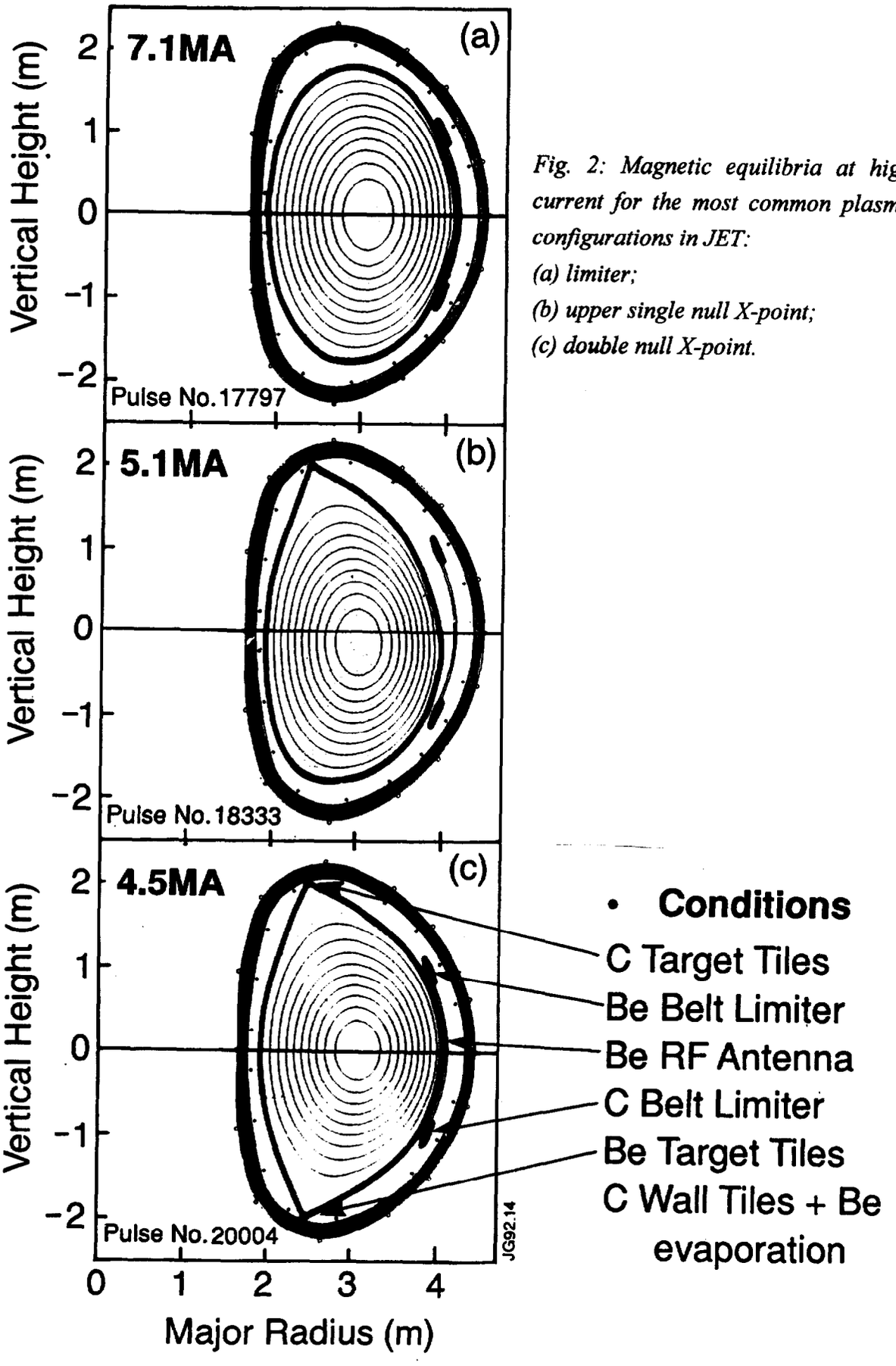

Fig. 2: Magnetic equilibria at high current for the most common plasma configurations in JET:
(a) limiter;
(b) upper single null X-point;
(c) double null X-point.

3. MHD Stability

Tokamak plasmas are subject to many types of mhd instability [4]:

- **Major disruptions** destroy the plasma, causing significant thermal and electromechanical stresses on the structure;
- **Vertical instability** of the plasma position produces very substantial electromagnetic forces on the vacuum vessel;
- **Sawteeth** limit the central plasma parameters, and hence the fusion power, and may cause rapid loss of α-particles;
- At beta (pressure) limits **ballooning modes** or **kink modes** can cause disruptions, or degrade confinement;
- **Fast particle driven modes, such as 'fishbones' or toroidal Alfven eigenmodes (TAE)** may degrade confinement and expel high energy particles;
- **Edge localized modes (ELM's)** enhance transport at the plasma edge in the H-mode, but may turn out to be benign by assisting the expulsion of impurities.

Major disruptions have been identified as having a variety of causes in JET. Principal amongst these are current rise instabilities, density limits, the low-q limit at q_ψ=2 and error field instabilities. In addition, there are several reproducible phenomena, such as large sawtooth collapses or pellet injection, which give rise to major disruptions, although the underlying reasons are not yet understood. Finally, vertical instabilities lead ultimately to a major disruption.

The evolution of the plasma towards a major disruption has been investigated in detail in JET [5]. Following an initiating event (see Fig. 3), such as those summarized above, mhd modes with low poloidal and toroidal mode numbers, m and n, are destabilized. In JET, an m=2, n=1 mode emerges as the dominant mode. This may have frequencies of up to 20kHz, determined largely by the plasma bulk rotation velocity and can grow at rates of up to $10^3 s^{-1}$. The mode locks to the vacuum vessel wall when the radial magnetic field, B_r, reaches ~10G and the disruption occurs with B_r~100G. Between the locking of the mode to the wall and the major disruption, a series of minor disruptions can occur which reduce the plasma energy, but do not lead to current decay. The major disruption, which is indicated by the occurrence of negative single turn loop voltage of ~100V, is accompanied by a rapid loss of the remaining plasma

energy and a quench of the plasma current, which can decay at rates of up to $10^9 As^{-1}$. The high loop voltage which occurs at the major disruption can generate runaway electrons with energies of 10's of MeV, which can damage plasma facing components. In addition, the large electromagnetic forces produced by the rapid decay of plasma current produces large stresses in the vacuum vessel. These two effects are a source of considerable concern for reactor operation.

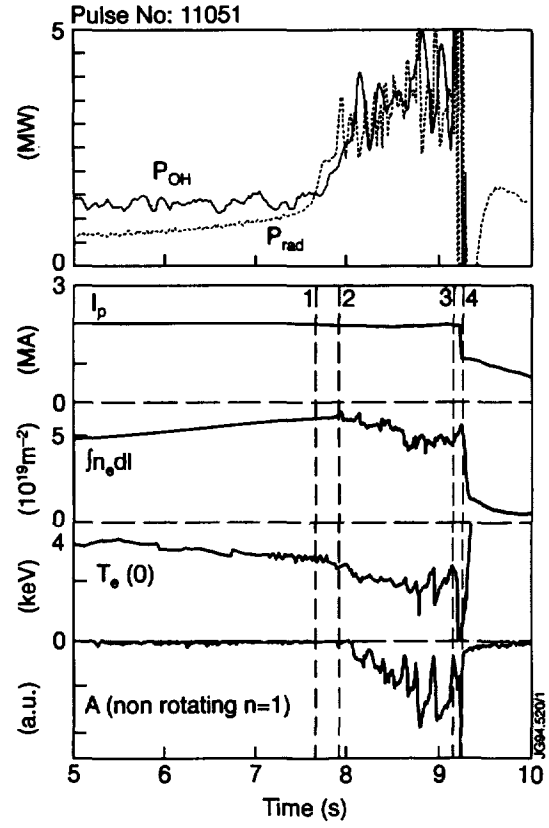

Fig. 3: Sequence of events leading to a density limit disruption
(1) $P_{rad}/P_{OH} \sim 1$;
(2) growth of mhd activity;
(3) m=1 erosion of profiles;
(4) energy quench and current decay.

It has been observed experimentally that there is a maximum density at which the tokamak can operate. Originally, it was found that, in ohmically heated plasmas, this density limit scaled with the plasma current and it was suggested that the limit was due to an imbalance between the input power, which also increases with current, and losses through impurity radiation. Detailed investigations in JET have confirmed this model and it has been shown that, for plasmas with low impurity content, that is Z_{eff}~1-2, the density limit scales with the square root of the total input power. This has confirmed the radiation model of the density limit in which cooling of the plasma edge due to impurity radiation leads to a contraction of the temperature profile away from the limiter. The increased resistivity at the plasma edge causes the edge current density to fall and the current profile eventually contracts within q_ψ=2, driving the m=2,n=1 mode unstable.

The introduction of beryllium into JET had a very marked influence on the density limit and the frequency of disruptions [3,6]. It was found that a MARFE, or asymmetric radiation

feature, occurred at the density limit, changing the particle transport properties at the edge and causing the density to fall. As a result the radiation was reduced and the major disruption often suppressed. Moreover when disruptions did occur, the rate of current decay was very much reduced as the plasma temperature was higher, closer to 100eV than the 10eV characteristic of carbon plasma facing surfaces, due to the changed nature of the impurity radiation with a beryllium limiter.

Current rise instabilities, as their name implies, occur as a result of phenomena which occur during the current rise. The reason for this can be understood in terms of the l_i-q_ψ diagram [7]. Fig. 4 illustrates this diagram in which a number of stability boundaries have been plotted. The upper boundary corresponds to the density limit: contraction of the current profile under radiation cooling causes the plasma inductance to rise until the plasma current flows entirely within q_ψ=2, leading to a stability boundary at high l_i. A second boundary has been found experimentally at q_ψ=2. The contribution to the stability boundary at low l_i is due to current rise instabilities, which grow when crossing integer values of edge q_ψ with a current profile which is too broad. The dangerous regions are indicated by the vertical lines at integer q_ψ. Fig. 4 shows the trajectory followed by a JET plasma during the current rise phase. As the trajectory crossed q_ψ=4,5,6 bursts of mhd activity were observed and the plasma eventually disrupted due to the mhd destabilized on crossing q_ψ=4.

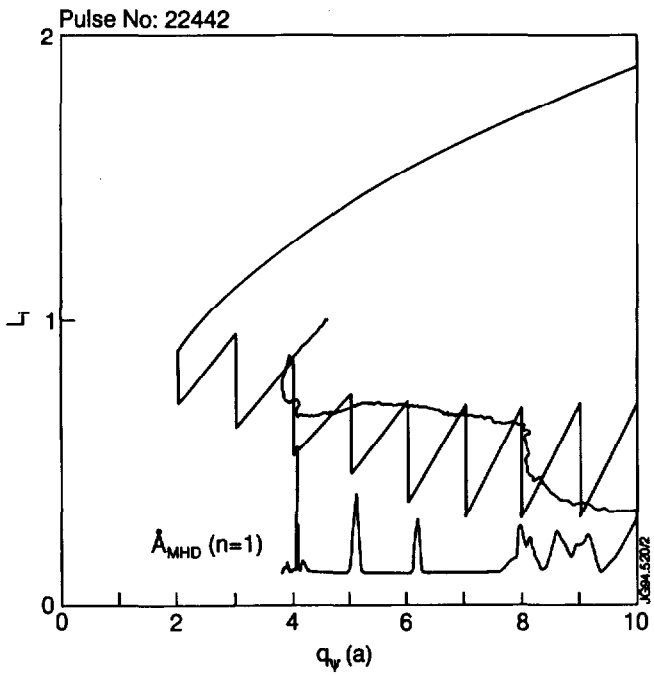

Fig. 4: Trajectory of a JET plasma in the l_i-q_ψ diagram in which various stability boundaries are indicated (see text). Also shown is a trace of the amplitude of rotating mhd activity observed during the evolution of the discharge. Note the bursts of activity at q_ψ=4,5,6.

In recent years a new and surprising cause of disruptions has been identified in large tokamaks. It was found in D-IIID [8], and confirmed in JET [9] and other devices, that small deviations from axisymmetry in the confining magnetic field structure can lead to the growth of mhd modes. These error fields arise from coil connections and small misalignments. In

JET, for example, an error field with an n=1 component of ~1G at the vacuum vessel wall leads to the growth of a mode with B_r~10-20G and this almost invariably leads to a disruption. Since the mode grows from a stationary field error, resistive tearing can occur only when the plasma is brought to rest. This manifests itself in a threshold density above which growth of the mode is suppressed by the intrinsic rotation of the plasma. Similarly, injection of angular momentum by NBI can be used to suppress the growth of such modes. Fig. 5 shows how the operating range in n_e and q_ψ is restricted in ohmic plasmas by this phenomenon. The figure also illustrates that the threshold is worse with the magnetic field helicity which matches that of the intrinsic error field. This is considered to be a significant problem for ITER, since it has been found, in agreement with theoretical expectations [10], that the magnitude of permissible error field diminishes with increasing tokamak size.

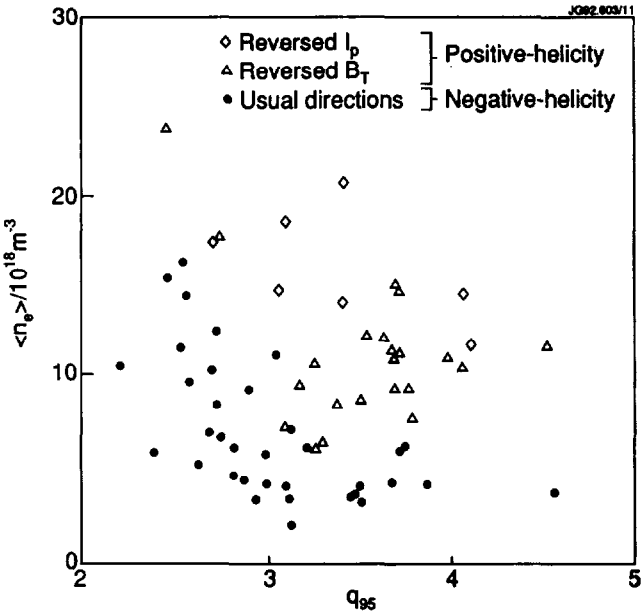

Fig. 5: Stability diagram for error field modes in the n_e-q_ψ plane. The points shown indicate where the growth of n=1 modes induced by an error field was observed for two helicities of the magnetic field. Note that the problem is more severe for one magnetic field helicity than the other.

As might be expected, the severe consequences of disruptions have led to the development of techniques for avoiding them or for ameliorating their impact. By making use of a knowledge of the stable operating regimes discussed above it is, in the main, possible to pilot a safe trajectory in the tokamak operating space. However, this is not invariably so and, even in a reactor, it is anticipated that a finite number of disruptions will occur. This has stimulated the exploration of techniques for reducing the severity of disruptions in situations where their occurrence is inevitable, ie once an m=2,n=1 mode has grown to locking amplitude, or ~10G in JET. For major disruptions initiated by a vertical instability little can be done at present as the instability growth rates are so rapid, attaining ~100s^{-1}. However, in all other cases, the disruption is preceded by the growth and locking of an m=2,n=1 mode. A detection system has, therefore, been established which uses the occurrence of this mode to initiate a plasma termination [11]. In particular the plasma current and elongation are reduced as rapidly as allowed by resistive dissipation and the inductances of the poloidal field circuits so as to

minimize the forces produced by the disruption. As shown in Fig. 6, this has succeeded in reducing the forces by an order of magnitude.

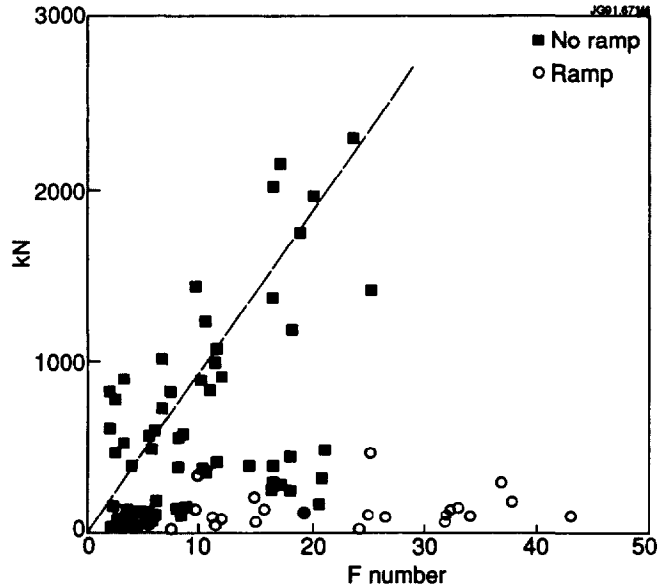

Fig. 6: Measured forces on the JET vacuum vessel caused by disruptions plotted against the pre-disruptive value of 'F-Number', a function depending on plasma current and elongation which expresses the theoretical severity of the disruption. It is clear that initiating plasma shutdown at the growth of an n=1 locked mode substantially reduces disruption forces, as discussed in the text.

The sawtooth instability is a second global mhd instability which can influence plasma confinement. Fortunately its effects are not as severe as the major disruption. It is associated with the growth of an mhd mode at the q=1 surface having a helical symmetry of m=n=1 and it leads to a rearrangement of plasma profiles about the q=1 surface. The instability flattens the central plasma profiles, redistributing energy and particles, including energetic particles, to radii outside the q=1 surface. It occurs as a repetitive instability in tokamak plasmas: the inward diffusion of current lowers the central value of q, q(0), and the instability leads to a redistribution of current, raising q(0). Sawteeth have been extensively studied in recent years, but there is no general agreement either on the experimental phenomenology of the sawtooth cycle, or on the theoretical explanation for the instability.

Fig. 7 illustrates the main phenomena associated with the sawtooth cycle in JET [12]. The 'full' collapse occurs as a rapidly growing instability, with growth rates ~$10^4 s^{-1}$, which flattens the plasma profiles across the entire region within q=1. In JET the growth rate of this instability is more than an order of magnitude too fast to be explained by the conventional, or Kadomtsev [13], model. However, alternative explanations, such as that proposed by Wesson [14], rely on q(0) remaining close to unity throughout the sawtooth cycle, a constraint which is contradicted by far-infrared polarimetric measurements of q(0) in JET and other machines [15]. Partial sawteeth have widely varying timescales, as indicated in the figure, but their common feature is that they affect the plasma temperature close to the sawtooth inversion radius, which is also believed to correspond approximately to the q=1 radius, much more strongly than at the plasma centre. Other m=n=1 modes such as 'fishbones' [16] are observed both in NBI heated discharges and, as in the figure, in ICRH plasmas.

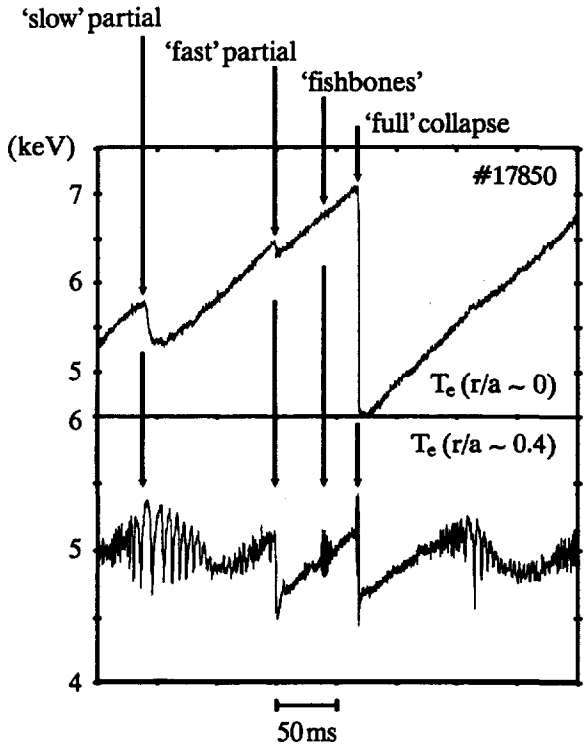

Fig. 7: Behaviour of the electron temperature at two radii during a sawtooth cycle in a JET discharge with ICRF heating. The major commonly observed phenomena are indicated.

There are several concerns associated with sawtooth activity in reactor plasmas. Clearly, such activity might limit the central plasma parameters which can be achieved, thereby limiting the fusion power. In addition, analysis of the sawtooth inversion radius, r_{inv}, generally finds that $r_{inv} \propto q_{\psi}^{\alpha}$, with $\alpha \sim -1$. This is particularly serious in reactor plasmas, which are expected to operate at values of $q_{\psi} \sim 3$, where the sawtooth inversion radius can correspond to $r/a \sim 0.5$. This suggests that a significant fraction of the plasma volume will be affected by sawteeth. Moreover, since the thermonuclear power varies as n^2T^2, sawteeth could cause an unacceptable modulation of the fusion reactivity and could present difficulties in controlling the 'burn'. Finally, sawteeth may scatter energetic α-particles from the plasma core before they have thermalized, reducing the thermonuclear heating efficiency. As a result, considerable efforts have been expended to investigate techniques for the stabilization of sawtooth activity, including current profile control, as discussed in section 5, and the use of fast particles [17].

To provide an economic source of energy, tokamak reactors must operate at the highest possible value of the plasma β_t, where $\beta_t = \langle p \rangle / (B_\phi^2 / 2\mu_0)$ and is the ratio of the average plasma pressure normalized to the toroidal field pressure. This is limited by a variety of mhd instabilities, principally ballooning and kink modes, and the precise limit depends on the details of the plasma current and pressure profiles. The most commonly quoted theoretical limit, that due to Troyon [18], is determined by the onset of high-n ballooning modes for optimized plasma profiles, and has a simple dependence on plasma parameters,

$$\beta_{Troyon}(\%) = 2.8 \times \frac{I_p}{aB_\phi}(MA, m, T), \qquad (1)$$

where I_p is the plasma current, a the minor radius and B_ϕ the toroidal magnetic field. Many tokamaks, including JET, have achieved β_t values close to this limit, the best value in JET being 6%, slightly above the predicted value [19]. It is not clear whether this will prove an absolute limit in JET as other tokamaks, in particular D-IIID [20], have achieved β_t values considerably in excess of this.

4. Confinement

Extensive investigations have been carried out of energy and particle confinement in L- and H-mode regimes. Local transport analysis has been performed both for steady-state plasmas using a variety of numerical codes (eg TRANSP [21]) and for transient conditions by exploiting a range of perturbative techniques. For example, by using the temperature and density perturbations created by sawteeth, not only have the electron thermal and particle diffusivities been measured, but the coupling between heat and particle transport has also been addressed [22]. In addition, specific experiments have studied the scaling of local transport coefficients with 'non-dimensional' parameters. This last study has shown that local heat transport in JET is better described by the 'Bohm' than the 'gyro-Bohm' formulation [23].

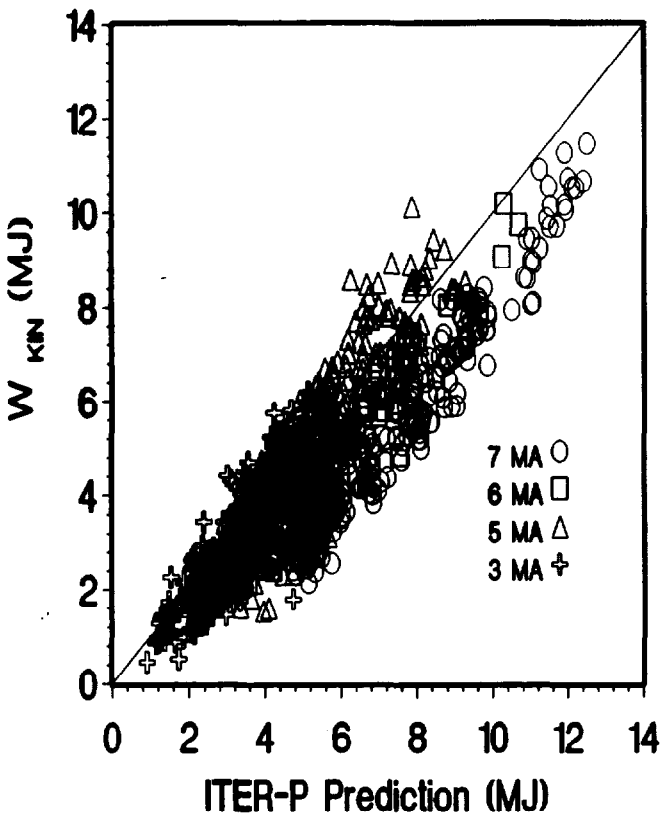

Fig. 8: Stored plasma energy, excluding fast particles, for L-mode plasmas in the range 3-7MA plotted against the predictions of the ITER-89P scaling law.

L-mode confinement is observed in both limiter and X-point plasmas, but the discussion here is limited to the former case, since this has been characterized over the widest parameter range of any tokamak. Experiments have been performed with currents ranging from 1 to 7MA, exploring a range of q_ψ values from 2 to 13. Heating schemes have included NBI, ICRF and LHCD, with total powers as high as 35MW. In the main, energy confinement varies as $I_p^{\alpha} P_{tot}^{-\beta}$, with $\alpha \sim 1$ and $\beta \sim 0.5$, which is characteristic of common scaling laws such as Goldston L-mode [24] or ITER-89P [25]. However, as shown in Fig. 8, at currents of 6-7MA, energy confinement times were below the scaling predictions [26]. One explanation for this behaviour is a reduction of central confinement due to sawteeth, which have a large inversion radius at the low q values (~3) typical in these high current plasmas.

In discharges with an internal separatrix, if the input power is above a threshold level the plasma can make a transition to a regime in which the confinement time approximately doubles [27]. The power requirement for this transition between L- and H-modes depends on a number of plasma parameters, but principally the magnitude and direction of the toroidal magnetic field. It is usually found that the threshold power increases approximately linearly with the magnitude of the toroidal field. In addition, the threshold power for plasmas in which the direction of the magnetic field is such that the vertical drift of ions due to the magnetic field gradient is towards the X-point is approximately half that for the case in which the ∇B ion drift is away from the X-point [eg 28]. In some tokamaks there is also evidence of an increase in threshold power with plasma density, but in JET this has not been observed to date.

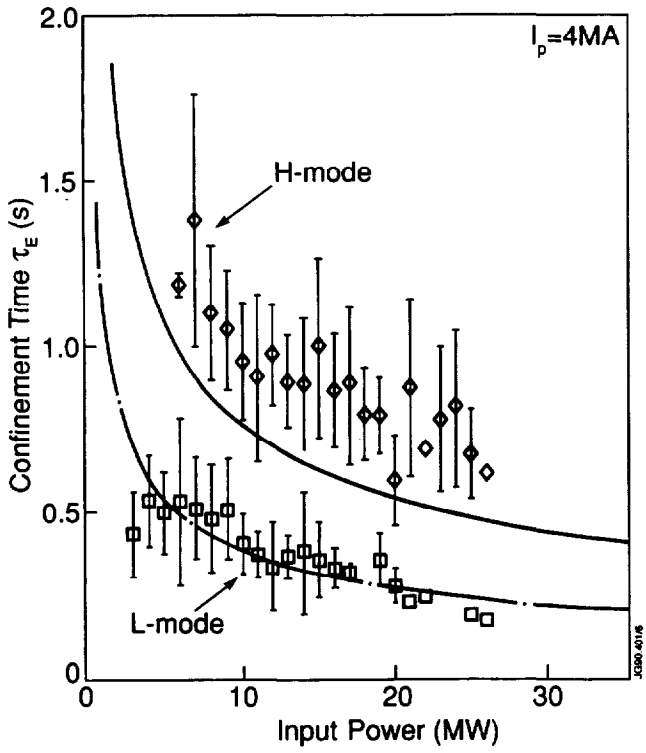

Fig. 9: Energy confinement time plotted against input power for a series of L and H-mode plasmas at 4MA. The broken line shows the prediction of the Goldston L-mode scaling law and the solid line is twice this law.

Fig. 9 compares the variation of global energy confinement times with increasing input power for two series of 4MA discharges: L-mode plasmas, limited by a material limiter, and H-mode plasmas which were bounded by an internal separatrix and which had input powers above the threshold power for the H-mode transition. The broken line shows the prediction of the Goldston L-mode scaling law for 4MA and the solid line corresponds to twice the Goldston law. Both sets of data exhibit the commonly observed degradation of confinement time with increasing input power, but the gain of at least a factor of two in confinement is maintained by the H-mode plasmas to the highest power levels. This gain is observed both in NBI and ICRF heated discharges and the power threshold for attaining the H-mode is similar in the two cases.

As in L-mode plasmas, there was some deviation from the prediction of scaling laws at the highest currents. Experiments were performed in the double-null X-point configuration (see Fig. 2) at currents of up to 5MA in both sawtoothing and sawtooth-free plasmas. It was found that up to ~4MA, the energy confinement time increased approximately linearly with plasma current, but that in the region 4-5MA there was little systematic improvement in confinement [29]. Comparison of data from sawtoothing and non-sawtoothing plasmas indicated that degradation of central confinement due to sawteeth did not explain this behaviour. One possible explanation is that at the highest currents in JET, due to limitations in the shaping current capability, the X-point was actually *outside* the target plates, so that formally the plasmas should be thought of as limiter plasmas limited on the top and bottom target plates. These discharges differ from conventional outer limiter plasmas in having a much higher shear at the plasma edge and a lower poloidal field at the top and bottom, near the X-points. Thus, they can still access the H-mode. Nevertheless, since much of the improvement in plasma energy and particle confinement in the H-mode is associated with the plasma edge, it is possible that the reduction of shear relative to a true X-point configuration was responsible for the reduction in confinement relative to the scaling laws (which are based on data from lower currents where good X-point configurations can be produced). A second possibility is that the observed degradation in plasma purity with increasing current played a role.

In many tokamaks, edge localized modes, or ELM's, are observed throughout the H-mode. As the name suggests, these instabilities occur in the plasma edge and they degrade the energy and particle confinement there. Their effect on particle confinement is, however, much greater than that on energy confinement, and their overall effect is now regarded as beneficial, since they allow the exhaust of impurities, which would include helium ash in a reactor, with a relatively small (~20%) penalty in energy confinement. In JET H-modes are generally ELM-free, with the result that the plasma density increases throughout the duration of the H-mode, leading to a monotonic rise in radiation which, after several seconds, causes the plasma to revert to the L-mode.

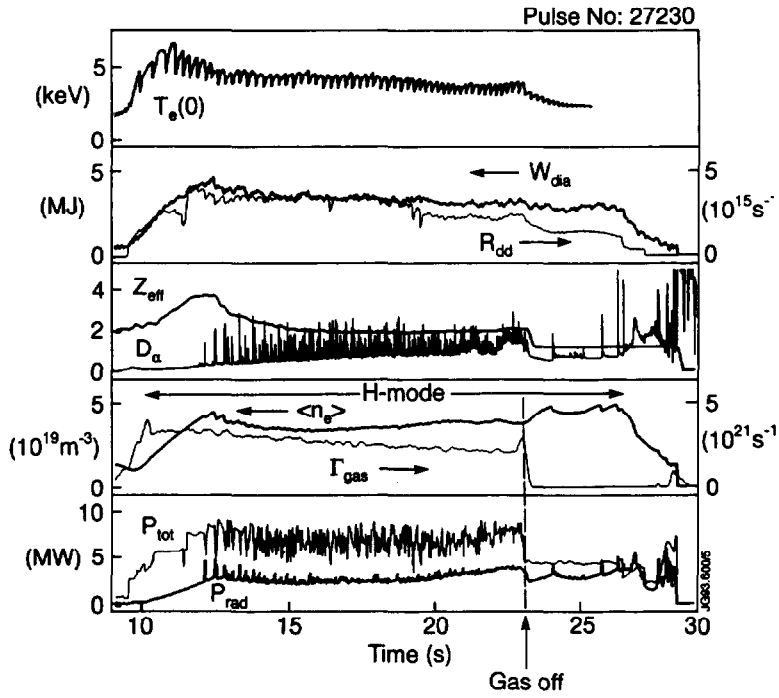

Fig. 10: Long steady-state ELMy H-mode produced by gas-puffing. When the gas-puff was switched off at ~23s the plasma reverted to an ELM-free H-mode.

While the energy confinement of such transient H-modes is high, the regime is unsuitable for reactor applications. Therefore, a series of experiments was performed to investigate means for producing ELM's. The most successful technique developed was the use of continuous gas-puffing during the H-mode. With gas puffs of $\sim 3\times10^{21}$at.s^{-1}, ELMy H-modes of up to 18s in duration were established [30]. Fig. 10. illustrates an example of shorter duration which shows that when the gas-puff was terminated at 23s, the plasma reverted to an ELM-free H-mode, with an increased density, despite the fall in input power at that time. It can be seen in the figure that, following a short ELM-free period, which is visible in the D_α signal, regular D_α spikes occurred, which are characteristic of ELM's. These persisted throughout the gas-puffing and during this time the main plasma parameters, including the impurity content, Z_{eff}, were held constant.

Analysis of the thermal energy confinement in these plasmas revealed that the best cases had a thermal energy content, that is excluding contributions from fast particles created by NBI or ICRF, equivalent to 95% of that predicted by the JET/D-IIID H-mode scaling, which was derived from confinement analysis of ELM-free H-modes in JET and D-IIID [31]. The dominant influence on energy confinement in these steady-state plasmas was found to be large amplitude n=1 mhd activity which proved unusually persistent and in some cases reduced the energy confinement to only 75% of that predicted by JET/D-IIID scaling. The cause of this

n=1 activity was not clear, but the modes were suppressed at the highest powers and those plasmas had energy confinement times corresponding to the higher value quoted here. Thus, this regime allows the maintenance of steady-state H-mode conditions with only a small loss of energy confinement.

5. Current Drive Experiments

In almost all tokamaks the plasma current is driven by inductive means, but a tokamak reactor will have to exploit alternative current drive techniques if steady-state operation is to be realized. A range of current drive issues have been explored in JET experiments, including techniques for enhancing the efficiency of steady-state current drive techniques using lower hybrid waves (LHCD), exploitation of the bootstrap current to reduce the requirements on other current drive techniques, and the investigation of current profile control techniques by fast wave current drive (FWCD) for stabilization of mhd instabilities.

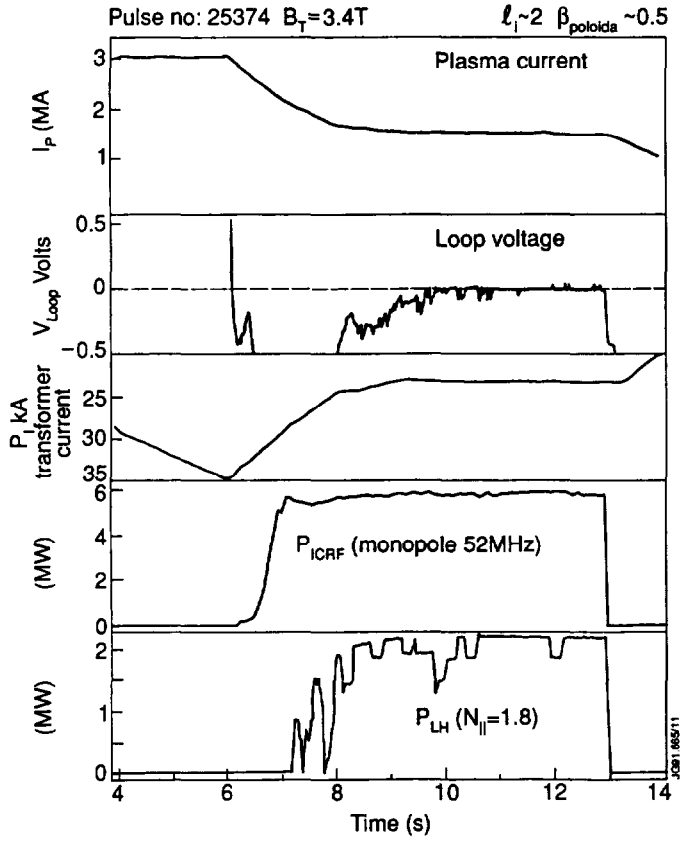

Fig. 11: Plasma parameters for a case in which 100% current drive was achieved.

In preliminary attempts to drive current by LHCD, the full plasma current has been driven for 6s at 1.5MA using 2MW of LHCD and 5MW of ICRH for plasma heating [32], as shown in Fig. 11. However, higher current drive efficiencies have been obtained in experiments in which synergistic effects between LHCD and ICRF have been exploited. It is thought that damping of the ICRF waves on energetic electrons produced by the lower hybrid waves can

accelerate them to higher energies, increasing the effective current drive. Evidence for this comes from measurements of bremsstrahlung produced by energetic electrons in such discharges. These show that in plasmas which attain full current drive, ie zero loop voltage, photon spectra with 'temperatures' of ~40keV are observed, while in cases where combined LHCD + ICRF are used the photon spectra yield 'temperatures of ~140keV. Experiments have shown that these 'synergistic' effects are increased in plasmas with low electron density, peaked density and temperature profiles and a large central fast electron population. In such cases current drive efficiencies, γ_{CD}, of up to $0.4\times10^{20}m^{-2}A/W$ have been achieved, where

$$\gamma_{CD}(m^{-2}A/W) = \frac{Rn_e I_{LH}}{P_{CD}}. \qquad (2)$$

R is the major radius, n_e the electron density, I_{LH} the driven current and P_{CD} the power necessary to drive this current.

An alternative approach to current drive exploits an effect of the transport processes which occur in a plasma confined in toroidal geometry. This effect, known as the bootstrap current, occurs as a result of the diamagnetic current carried by electrons 'trapped' in 'banana' orbits on the large major radius side of the plasma [33]. Collisions between the trapped and passing electrons gives rise to a current carried by the passing particles, the resultant current density, $j_{bootstrap}$, being given approximately by,

$$j_{bootstrap} \approx -\varepsilon^{1/2} \frac{1}{B_\theta} \frac{\partial p}{\partial r}, \qquad (3)$$

where ε=a/R, B_θ is the poloidal magnetic field and $\partial p/\partial r$ the gradient of the plasma pressure with respect to the minor radius. A more precise expression can be found in the collisionless and large aspect ratio limits and this can be integrated, by assuming simple forms for the plasma density and temperature profiles, to yield an expression for the total bootstrap current, $I_{bootstrap}$,

$$I_{bootstrap} \approx 0.7\varepsilon^{1/2}\beta_p I_p, \qquad (4)$$

where β_p is the ratio of the plasma pressure to the poloidal field pressure, $\beta_p = < p > /(B_\theta^2 / 2\mu_o)$. The major advantage of this form of current drive is that no additional source of power is necessary beyond that required to heat the plasma. Moreover, in a reactor, most of this power would be produced by the fusion reactions. This is potentially, therefore, an extremely efficient form of current drive.

In experiments in JET, ICRF heated plasmas at 1MA/2.8T have attained β_p values of ~2, resulting in 70% (±15%) of the plasma current being driven by the bootstrap effect [34]. In Fig. 12, which shows the analysis of the loop voltage from such a discharge, it can be seen that only by including the bootstrap effect can the calculated voltage at the plasma surface be brought into agreement with the measured value. These plasmas did not attain steady state and the high confinement regime collapsed after several seconds for unknown reasons. An intriguing aspect of these H-mode plasmas is that their thermal energy confinement time is substantially better than predicted by conventional H-mode scaling laws, reaching ~1.7 times the value predicted by the JET/D-IIID scaling. Further experiments are required to investigate whether steady-state operation can be achieved in this regime and to determine if the enhanced confinement is associated with the high values of β_p, modification of the current profile by the bootstrap current, or some as yet unidentified effect.

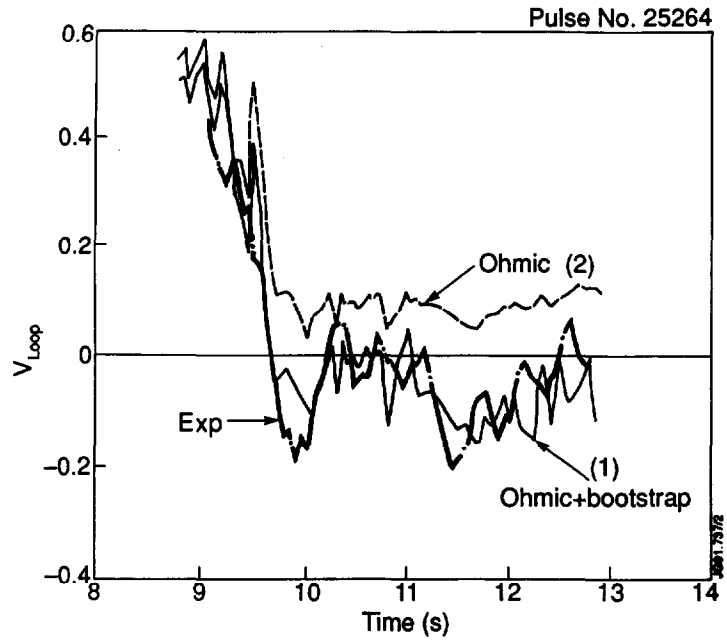

Fig. 12: Comparison of the measured (Exp) and calculated values of the loop voltage for a discharge in which 70% of the current was driven by the bootstrap current. Only by including contributions from both the ohmic current and the bootstrap current could good agreement between the calculations and experimental measurements be achieved.

A third technique for the production of non-inductive current exploits the launching of directed waves by the ICRF system. Phasing of the elements of the ICRF antenna array produces an asymmetric parallel wavenumber spectrum and the interaction of the waves with either electrons or minority ions can drive current [35]. Minority ion current drive has the particularly interesting feature that current is driven in opposite directions on either side of the minority ion resonance. As a result there is little net current drive, but the change in the current density profile which is produced can have a significant impact on the mhd stability of the plasma if the resonance position is appropriately chosen.

This technique has been applied at the q=1 surface in JET with dramatic effects on the behaviour of sawteeth [36]. Fig. 13 compares the effect on the sawtooth activity of several ICRF heating schemes with the minority resonance located at a radius corresponding to the

q=1 surface. In the normal case (labelled dipole and corresponding to a 180° phasing of the antenna current straps) rapid sawteeth of large amplitude were produced. When the phasing was changed to -90°, the sawtooth frequency increased to such an extent that their amplitude was reduced almost to zero. By contrast, when +90° phasing was used, the period and the amplitude of the sawteeth increased. These results are consistent with the expectations of RF current drive theory in which the -90° phasing should drive currents which increase the gradient of the current density profile at the q=1 surface, and which, on the basis of certain theories of the sawtooth instability, should *destabilize* sawteeth. The +90° phasing, on the other hand, is expected to drive currents which decrease the gradient of the current density profile, *stabilizing* sawteeth. These initial experiments may offer a route to the stabilization of sawteeth in a reactor.

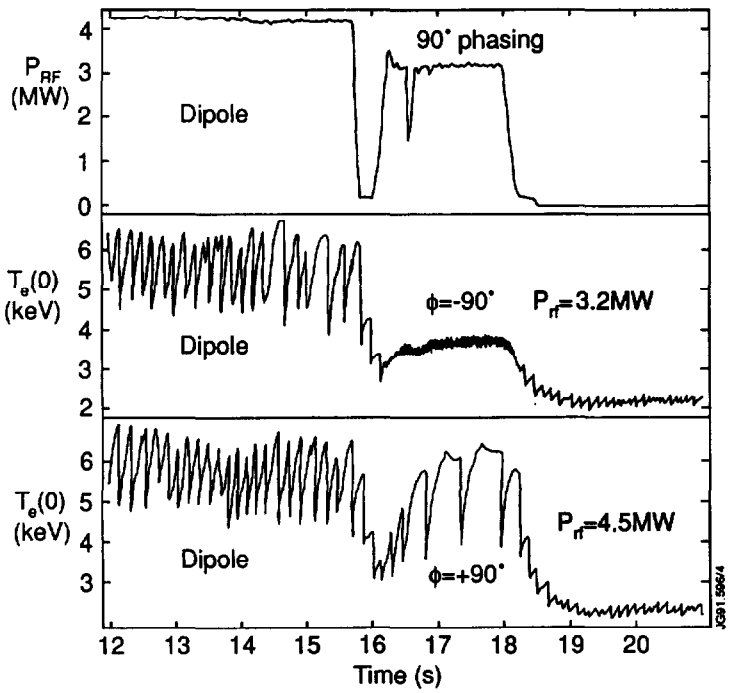

Fig. 13: Demonstration of ICRF current drive via minority ions through its effect on sawtooth activity. The minority resonance was located at the q=1 radius as determined from the sawtooth inversion radius.

6. Summary

Tokamak plasmas are subject to a wide range of mhd instabilities of varying degrees of severity. Of these the major disruption and the vertical instability are likely to pose the major threats to the integrity of a fusion reactor due to the severe forces imposed on the machine structure. Identification of the operational boundaries for the occurrence of these instabilities is the subject of continuing experiments at JET, and at many other tokamaks, and techniques for their control are being developed. There are two quite general confinement regimes, known as L-mode and H-mode. In the latter case energy confinement is usually a factor of 2 greater than in L-mode. Moreover, under special conditions energy confinement can be enhanced beyond the normal H-mode level, but to date such regimes have been transient and

much further experimentation is required to identify whether reactor plasmas can be maintained in steady-state in such regimes. Steady-state operation of a reactor will require that the current be driven by non-inductive means. A variety of methods such as bootstrap current, LHCD and FWCD could contribute to current drive and experiments have been performed which confirm the viability of these techniques for reactor-relevant parameters.

References

[1] *The JET Project - Design Proposal*, EUR-JET-R5, CEC, Brussels, 1975.

[2] The JET Team (presented by J Jacquinot), Plasma Phys. and Contr. Fusion **33** 1657 (1991).

[3] The JET Team (presented by K J Dietz), Plasma Phys. and Contr. Fusion **32** 837 (1991).

[4] J A Wesson, *Tokamaks*, Oxford University Press, Oxford 1987.

[5] J A Wesson et al, Nucl. Fusion **29** 641 (1989).

[6] The JET Team (presented by D J Campbell), Plasma Phys. and Contr. Fusion **32** 949 (1991).

[7] J A Snipes et al, Nucl. Fusion **28** 1085 (1988).

[8] J T Scoville et al, Nucl. Fusion **31** 875 (1991).

[9] G Fishpool and P S Haynes, Nucl. Fusion **34** 109 (1994).

[10] R Fitzpatrick and T C Hender, Phys. Fluids B **3** 644 (1991).

[11] G Saibene et al, Proc. IAEA Tech. Comm. Meet. on *Disruption Avoidance and Control*, Culham, September 1991, **1** 1.

[12] The JET Team (presented by D J Campbell), in *Plasma Physics and Controlled Fusion Research 1988* (Proc. 12th Int. Conf., Nice, 1988) Vol. 1, IAEA, Vienna (1989) 377.

[13] B Kadomtsev, Fiz. Plazmy **1** 710 (1975).

[14] J A Wesson, Plasma Phys. and Contr. Fusion **28** 243 (1986).

[15] H Soltwisch et al, in *Plasma Physics and Controlled Fusion Research 1986* (Proc. 11th Int. Conf., Kyoto, 1986) Vol. 1, IAEA, Vienna (1987) 263.

[16] K McGuire et al, Phys. Rev. Lett. **50** 891 (1983).

[17] The JET Team (presented by D J Campbell), in *Plasma Physics and Controlled Fusion Research 1990* (Proc. 13th Int. Conf., Washington, 1990) Vol. 1, IAEA, Vienna (1991) 437.

[18] F Troyon et al, Plasma Phys. and Contr. Fusion **26(1A)** 209 (1984).

[19] D Stork et al, Proc. 19th Euro. Conf. on Contr. Fusion and Plasma Phys., Innsbruck, 1992, **1** 339.

[20] L Lao et al, in *Plasma Physics and Controlled Fusion Research 1992* (Proc. 14th Int. Conf., Würzburg, 1992) Vol. 1, IAEA, Vienna (1993) 565.

[21] R J Goldston et al, J. Comput. Phys. **43** 61 (1981).

[22] G M D Hogeweij et al, Proc. 17th Euro. Conf. on Contr. Fusion and Plasma Phys., Amsterdam, 1990, **1** 158.

[23] The JET Team (presented by J G Cordey), in *Plasma Physics and Controlled Fusion Research 1992* (Proc. 14th Int. Conf., Würzburg, 1992) Vol. 2, IAEA, Vienna (1993) 161.

[24] R J Goldston, Plasma Phys. and Contr. Fusion **26(1A)** 87 (1984).

[25] P N Yushmanov et al, Nucl. Fusion **30** 1999 (1990).

[26] The JET Team (presented by P J Lomas), in *Plasma Physics and Controlled Fusion Research 1992* (Proc. 14th Int. Conf., Würzburg, 1992) Vol. 1, IAEA, Vienna (1993) 181.

[27] F Wagner et al, Phys. Rev. Lett. **49** (1408) 1982.

[28] D J Ward et al, Proc. 18th Euro. Conf. on Contr. Fusion and Plasma Phys., Berlin, 1991, **1** 353.

[29] T T C Jones et al, Proc. 19th Euro. Conf. on Contr. Fusion and Plasma Phys., Innsbruck, 1992, **1** 3.

[30] P R Thomas et al, ibid **1** 239.

[31] D P Schissel et al, Nucl. Fusion **31** 73 (1991).

[32] The JET Team (presented by C Gormezano), in *Plasma Physics and Controlled Fusion Research 1992* (Proc. 14th Int. Conf., Würzburg, 1992) Vol. 1, IAEA, Vienna (1993) 587.

[33] R J Bickerton et al, Nature Phys. Sci. **229** 110 (1971).

[34] C D Challis et al, Nucl. Fusion **33** 1097 (1993).

[35] V P Bhatnagar et al, JET Preprint JET-P(94)22 (to be published in Nucl. Fusion).

[36] D F H Start et al, Proc. 19th Euro. Conf. on Contr. Fusion and Plasma Phys., Innsbruck, 1992, **2** 897.

The JET Programme II:

Edge Physics, Fusion Performance and the New Phase of JET

D J Campbell
JET Joint Undertaking, Abingdon, Oxon, OX14 3EA, UK

Abstract

Extensive experiments have been performed to investigate plasma-wall interactions and the physics of the plasma edge. In particular, the relative merits of carbon and beryllium as first wall materials have been studied in some detail. High performance plasmas have been developed in which the projected fusion output power would be equal to the input power in a 50:50 deuterium/tritium plasma and these have been exploited to provide the first demonstration of fusion power production with a DT mixture. A new phase of JET has just begun following the installation of a Pumped Divertor. This is expected to offer better control of the plasma-wall interaction and to allow key questions relating to the design of a divertor for ITER to be addressed.

1. Introduction

As noted in the previous lecture, the study of plasma-wall interactions in plasmas with parameters relevant to a reactor is one of the fundamental goals of the JET project. As the fusion programme has evolved in the last decade, and a satisfactory characterization (if not understanding) of the processes governing stability and confinement has developed, the problems associated with the dissipation of the exhaust power and the control of particle flows in a reacting plasma have emerged as key issues in the development of a prototype fusion reactor such as ITER. In JET, these questions have assumed increasing importance to such an extent that the new phase of the JET experiment, which has just begun, involves the installation and operation of a Pumped Divertor which is designed to allow better power handling and improved control of deuterium and impurity fluxes in the plasma.

Since JET is expected to demonstrate significant α-particle heating in the final phase of DT experiments scheduled for 1996, the development of plasma regimes capable of producing substantial fusion power has become a central theme in JET experiments. The successes (and limitations) of this programme were exemplified in the preliminary tritium experiment (PTE) in which a DT mixture was used for the first time in a tokamak, leading to the production of

over 1MW of fusion power [1].

2. Edge Physics

Development of a satisfactory solution to the problems associated with the interface between the plasma and the first wall is now regarded as crucial to the construction of a fusion reactor. This lecture is concerned with the practical consequences of these concerns, while the underlying physics considerations are discussed elsewhere in this course [2] and in [3]. Principal amongst these problems is to develop means of dissipating the high power fluxes which will flow into the narrow 'scrape-off layer' (SOL) and towards the power handling surface (divertor target or limiter). A simple calculation shows that, in a reactor, power loads of 10's of MWm^{-2} are possible, while loads much above $\sim 5MWm^{-2}$ are considered unacceptable, as thermal stresses and erosion would be intolerably high. Moreover, transient loads, resulting from mhd instabilities for example, as well as steady-state loads must be considered.

The control of particle fluxes in a reacting plasma also presents significant difficulties. Not only must adequate fuel be supplied in the appropriate concentrations, but He ash must be exhausted and impurities generated by sputtering of the first wall must be prevented from reaching the main plasma. This last is particularly crucial as the dilution due to impurities (including helium) reduces the overall fusion power gain of a reactor and could, in the worst case, prevent ignition. Although there is still some debate on the issue, it is likely that a divertor rather than a limiter configuration will be chosen for the first reactors since the former offers advantages in particle control and in bulk plasma confinement over the latter.

In JET considerable emphasis has been placed on the selection of an appropriate material for the first wall and divertor target of a reactor. A suitable material must have high thermal conductivity, high resistance to thermal and mechanical shock and to neutron damage, low sputtering and erosion rates, and low radiation rates when ionized. As a result of this last requirement, low-Z materials such as carbon or beryllium are generally favoured for this application, since the plasma can tolerate higher concentrations than for high-Z materials such as tungsten or molybdenum.

Extensive experiments in recent years have compared the properties of carbon (either as graphite or carbon fibre composites, CFC) and beryllium both as limiter and divertor target materials [eg 4, 5, 6], examining not only the mechanical properties of the materials but also the impact of their use on the properties of the bulk plasma. For example, as discussed in the previous lecture, the use of beryllium limiters had a substantial impact on the behaviour at the density limit. The first wall configuration for the 1991-92 experimental campaign is illustrated

in Fig. 1 together with the upper (solid line) and lower (dashed line) single null X-point equilibria used to characterize the performance of the upper (CFC) and lower (Be) divertor targets. Note that none of the plasma-facing surfaces in present tokamak experiments are actively cooled, so that the temperature of surfaces interacting with the plasma rise uncontrollably during the plasma pulse. In this respect current experiments differ significantly from a reactor.

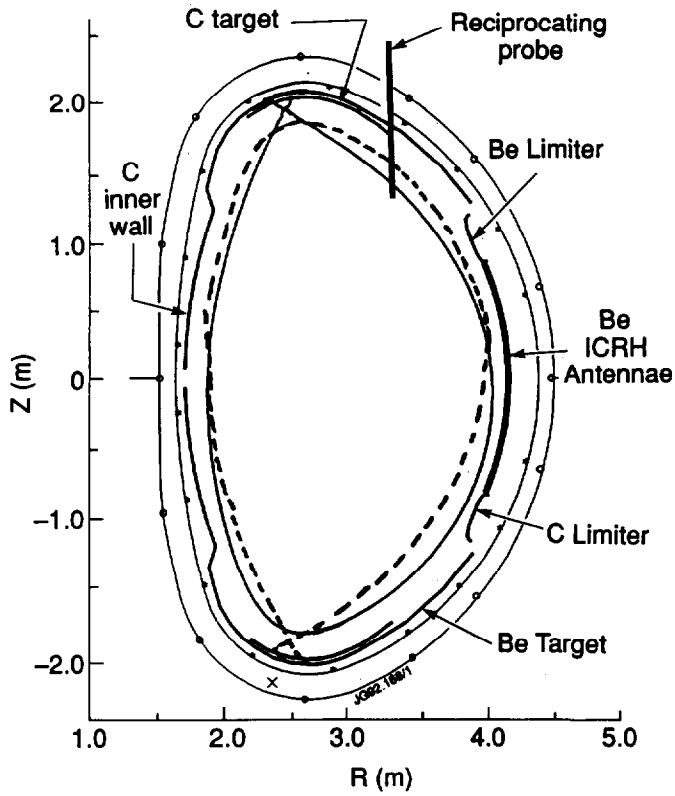

Fig. 1: Configuration of the JET first wall for the 1991-92 experimental campaign, showing the distribution of plasma facing materials. The standard upper (solid line) and lower (dashed line) single null X-point equlibria are also shown.

Beryllium was used initially in JET as a getter material, layers of ~100Å being applied by evaporation. This led to a significant reduction in Z_{eff} to ~1.5, with a substantial reduction in the carbon concentration. However, the reduction in oxygen concentration, which fell by more than an order of magnitude, was even more striking and was beneficial both in reducing the radiation loss from the plasma and in reducing the sputtering of nickel. A second major benefit arising from the use of beryllium, both as a getter and in metallic form as the limiter surface, was an improvement in particle control due to the efficient pumping of hydrogen isotopes by beryllium. As a result beryllium has been exploited extensively in JET experiments as a getter material and as a plasma facing surface

The understanding and avoidance of the carbon or beryllium 'bloom' [7] has been a major concern in JET experiments. The terminology arises from the fact that cameras viewing the carbon power handling surfaces 'bloom', ie saturate, when the surface reaches sublimation temperature (2700°C) due to the intense emission of carbon light from the sublimated

impurities. In such cases the Z_{eff} of the main plasma rapidly reaches values of ~6. Observations of localized heating revealed that small misalignments of target tiles, on the order of 1mm, caused exposure of tile edges to the incident power flux and, for the low angles of incidence characteristic of divertor geometries, this produced high power loads and a rapid rise in temperature. As a result considerable care has been taken to improve the shielding of tile edges by machining of the tiles and by improvements in installation procedures. This improved the power handling capability of the JET divertor target [8], as illustrated in Fig. 2, where the power handling capability of the Mk I target, in which the tile edges were not machined, is compared with that of the Mk II target, in which the tiles were machined. The significant rise in conducted energy to the target required to produce the carbon bloom in the Mk II target is evidence of the role played by localized heating of tile edges in the Mk I target and of the benefits which can be gained by careful machining and alignment.

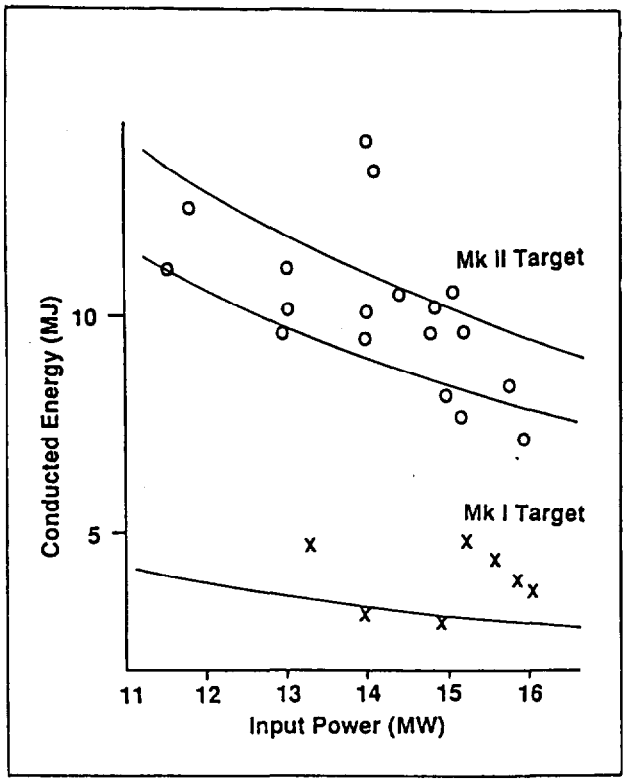

Fig. 2: A comparison of the power handling performance of the MkI and MkII CFC divertor targets used during the 1991-92 experimental campaign. This illustrates the advantages gained from profiling the MkII target tiles to hide edges.

Similar observations have been obtained for beryllium plasma facing surfaces, though, more seriously, beryllium melts at 1270°C. The beryllium divertor target was, therefore, unsuitable for use in the low density, high power discharges used to produce high fusion yield (see Section 3). However, at moderate densities, H-mode performance on beryllium did not differ greatly from that on carbon [6]. This was true even after extensive melting of the beryllium target had occurred. Fig. 3 compares the impurity influxes and bulk plasma impurity concentrations observed using the carbon (CFC) and beryllium divertor targets under a variety of conditions. When the low density regime is excluded, since the beryllium target was raised to melting temperatures in this case, it can be seen that the Be influx was approximately a

factor of 3 above the C influx, in reasonable agreement with expectations based on the plasma parameters and on the behaviour of Be and C sputtering as a function of divertor temperature (see figure inset). However, the Be content of the plasma exceeded the C content by only 50%, so that the dilution factors were similar. This apparent inconsistency between the divertor influxes and impurity content for the two materials might be explained by the observed additional influxes from other areas of the tokamak wall which are predominantly covered in carbon.

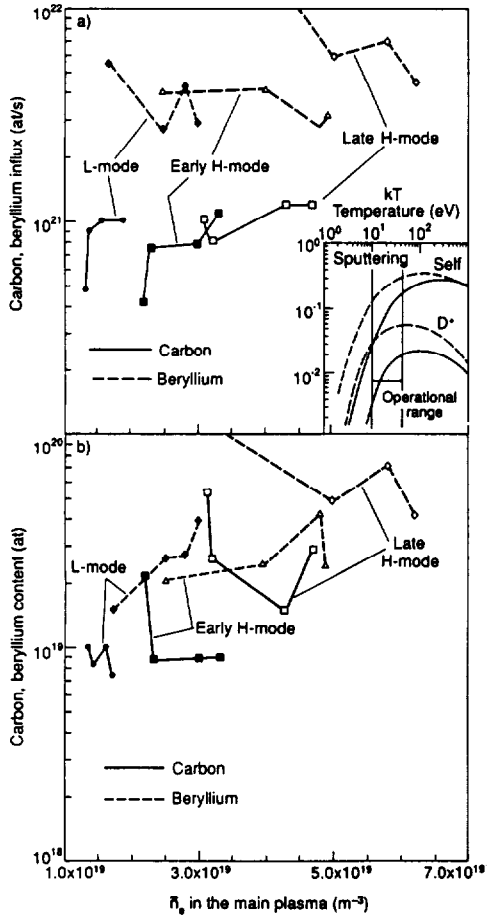

Fig. 3: (a) Comparison of carbon and beryllium influxes from the respective targets. (b) Comparison of the carbon and beryllium content of the plasma for the same discharges. Both graphs are plotted in terms of the volume averaged density of the plasma.

To mitigate the power handling problem in a reactor, a concept has been developed in which the power flowing to the divertor is dissipated by a combination of radiation and charge exchange, with a high density neutral gas region in front of the divertor target, the so-called 'gas target' [9, 10]. The emphasis in current edge and divertor studies is, therefore, the exploration of plasma operating regimes with high divertor density.

Initial experiments to explore these ideas have demonstrated the feasibility of establishing such a divertor regime, though further development is required [6, 11]. Fig. 4 shows a case in which a 3MA plasma diverted onto the Be target was established with ~20MW of input power. As a result of strong gas puffing, it was possible to dissipate approximately 95% of the input power by radiation and charge exchange, so that only ~5% of the power was conducted to the divertor target. The target temperature was then brought into steady-state at a

temperature of ~1000°C. This result demonstrates that such a regime is practical. However, the resultant bulk plasma exhibited energy confinement which was less than 40% above that predicted by L-mode scaling. Further experiments are required to investigate the compatibility of such divertor regimes with steady-state enhanced confinement in the bulk plasma and this will be a central theme of the new phase of JET involving the Pumped Divertor.

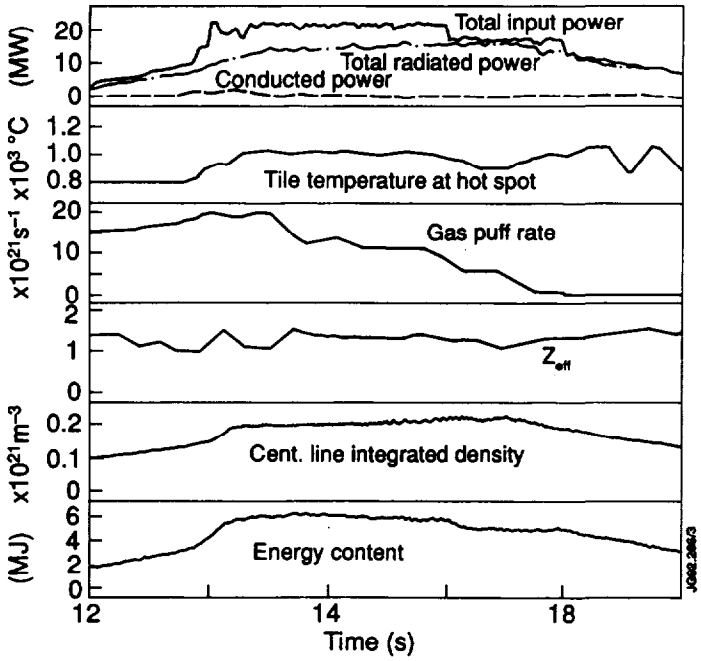

Fig. 4: Overview of a plasma discharge in which a 'gas target' divertor regime was established by strong deuterium gas puffing.

3. High Fusion Yield

JET high performance plasmas may be divided into two classes, broadly characterized as 'high-β_p' [12] and hot-ion H-mode [13]. The fusion performance of such discharges is usually characterized by the 'fusion triple product', $n_i(0)\tau_E T_i(0)$, where $n_i(0)$ and $T_i(0)$ are the central deuterium density and temperature respectively. It can be shown that for common profile shapes, the triple product is a good measure of the fusion potential of an equivalent plasma with a 50:50 deuterium/tritium mixture. In particular, $n_i(0)\tau_E T_i(0)=1\times10^{21}m^{-3}skeV$ corresponds to 'scientific breakeven', where the fusion power equals the plasma input power, and $n_i(0)\tau_E T_i(0)=6\times10^{21}m^{-3}skeV$ corresponds to ignition.

For completeness, a third high fusion power regime should be noted. This exploits the acceleration of ^3He minority ions to high energies by ICRF waves and produces fusion power via the D(^{3}He) reaction [14],

$$D + {}^3He \rightarrow H\ (14.7MeV) + {}^4He\ (3.6MeV) \qquad (1)$$

Until the PTE produced over 1MW of fusion power, the 100kW produced in JET via this

reaction represented the highest real fusion power attained in a tokamak.

Plasmas in which high global values of β_p were obtained were discussed in the previous lecture. However, 'high-β_p' also includes a class of discharges with high core values of β_p, known as 'PEP+H-modes', in which $n_i(0)\tau_E T_i(0)$ values of up to $7\times10^{20}m^{-3}$skeV have been achieved [15] ('PEP' represents pellet enhanced plasma). As shown in Fig. 5, this regime is formed by a combination of pellet injection, which produces a peaked density profile, and high power central heating, generally ICRH. The effect of the central heating is to freeze the current profile with the central q value, q(0), above unity. In addition, as the central pressure increases, a substantial bootstrap current develops, which produces a hollow q profile in the plasma core. It is thought that the resultant magnetic shear reversal may be responsible for the enhanced central confinement which is observed. However, like all high performance regimes, the PEP+H-mode is transient and decays on a timescale of 1-3s, the decay being accompanied in many cases by global mhd activity with toroidal mode numbers n=1,2,3.

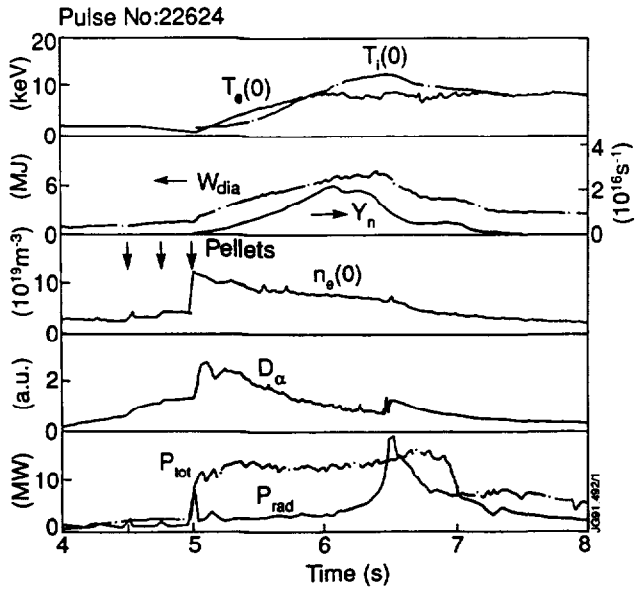

Fig. 5: Overview of a 'PEP+H-mode' plasma in which high power heating is applied after a peaked density profile has been formed by pellet injection.

The more general high fusion performance regime in JET is the hot ion H-mode. This is produced by high power NBI, in a few case combined with ICRF, in low target density plasmas, $\langle n_e\rangle<2\times10^{19}m^{-3}$, in a well conditioned torus. Low recycling conditions are crucial and these are generally produced by beryllium evaporation. Both single and double null plasmas are used, but the former has come to be favoured as, with the ∇B ion drift away from the divertor target, a more favourable distribution of exhaust power between the inner and outer divertor targets is obtained, which prolongs the high performance phase. In this regime, the thermal energy confinement is enhanced by up to a factor of 2 above the JET/D-IIID scaling [16]. These plasmas produce the highest values of the fusion triple product obtained in JET, with $n_i(0)\tau_E T_i(0)=9\times10^{20}m^{-3}$skeV, equivalent to $Q_{DT}\sim1$, or 'scientific breakeven'. An overview of such a discharge is shown in Fig. 6.

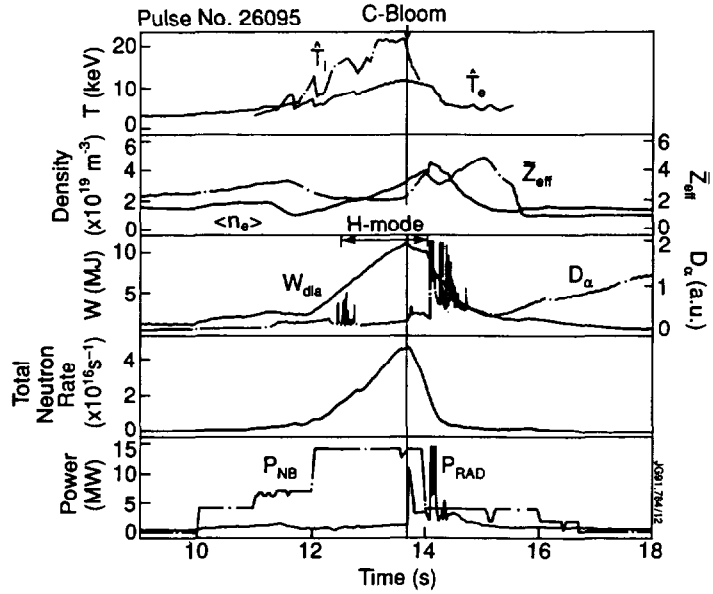

Fig. 6: Overview of a hot ion H-mode plasma in which a regime with high fusion performance is formed by injecting high power NBI into a low density target plasma.

The high performance phase of these discharges lasts for up to 1.7s, with the plasma parameters evolving throughout. In particular, the density rises from a low target value to central values of ~5×10^{19}. Central ion temperatures attain values in the range 18-25keV with very peaked profiles, while the central electron temperature rises to 10-12keV. High edge temperatures, in the range of several keV, are a feature of this regime [17]. Transport analysis shows that there is a considerable reduction of ion thermal conductivity across the entire plasma cross-section[18]. This is particularly significant in the plasma centre, as shown in Fig. 7, which compares the gradient in ion temperature at r/a=0.3 with the power flowing to the ions for various types of plasma. From this data, a simple evaluation of the ion thermal diffusivity, χ_i, is inferred for the various regimes. In hot ion H-modes and PEP+H-modes, this value of χ_i is reduced by a factor of 2 relative to standard H-modes [19].

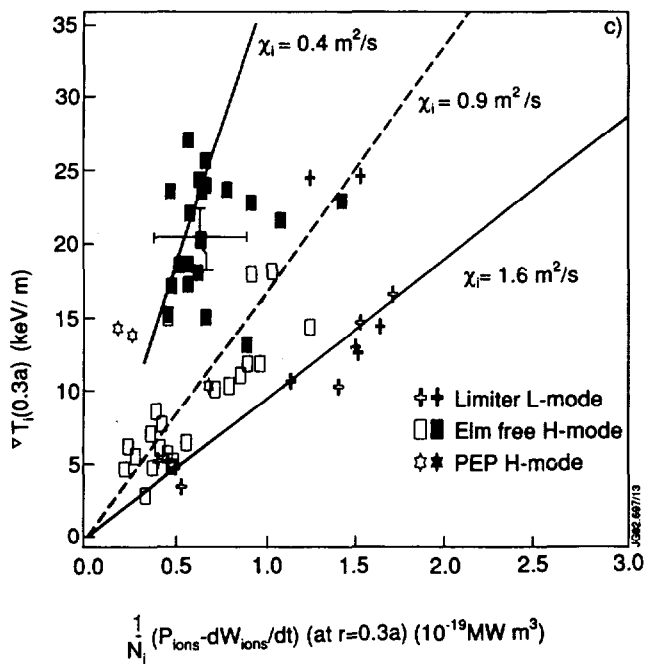

Fig. 7: Ion temperature gradient at r/a=0.3 versus ion heating power for various regimes in JET. The solid symbols represent hot ion plasmas (L-modes and H-modes). Lines representing inferred values of χ_i indicate the reduced ion transport in the hot ion H-modes.

The reason for the eventual decay of the high fusion performance in these plasmas is a key question which remains unresolved. There is considerable mhd activity, dominated by 'fishbone'-like bursts, during the high performance phase and there is some evidence that these bursts may reduce the rate of rise of central ion temperature. However, they have no observable impact on neutron emission and do not affect the global energy confinement. The termination of the high performance phase is often accompanied by global mhd activity such as an ELM or a sawtooth coupled to an ELM, but this is not invariably so and it is these cases in which there is no detectable mhd activity which are most revealing.

Fig. 6 shows the global plasma behaviour at the termination, which is indicated by the vertical line just before 14s. There is a sudden fall in the central ion temperature and in the global neutron yield while Z_{eff} and the radiated power rise suddenly. The central electron temperature and the stored energy, however, decay more slowly. Closer inspection of the data shows that there is also a sudden rise in plasma density and in D_α recycling light. It appears that the crucial event in the termination is a rapid (several ms) loss of confinement in the outer half of the plasma, which is clearly observed in the edge electron temperature. This is responsible for a sudden heat pulse to the divertor, which raises the target tile temperature from ~1500°C to ~2700°C and produces a carbon bloom. The resultant influx of impurities, coupled with a rise in core plasma transport, which allows the impurities to penetrate rapidly, leads to the very rapid fall in fusion performance. However, there is a second effect associated with the confinement loss, which is a rapid fall in core ion confinement. This effect is not understood and the precise relationship between the collapse in central ion temperature and the loss of edge confinement is difficult to establish because of the slower time resolution of the T_i diagnostic. However, the rapid fall in ion temperature makes a significant contribution to the loss of fusion power as over 50% of the neutron production is thermal. In cases where global mhd is implicated in the termination, the sequence of events is very similar, but the main difference is that the mhd event, either an ELM or a sawtooth plus an ELM, triggers the loss of edge confinement.

The fusion performance of JET plasmas is summarized in Fig. 8, in which the fusion triple product is plotted against the central ion temperature for various high performance regimes. Shaded bands correspond to equivalent values of Q_{DT} in a plasma with a 50:50 deuterium/tritium mixture. It can be seen that the best discharges lie in the region Q_{DT}~1. Many of the these lie in the hot ion regime, defined by

$$n_i(0)\tau_E T_i(0) < 4.6\times10^{17} T_i^{5/2}(0), \qquad (2)$$

in which the ions are effectively decoupled from the electrons. Since, in a reactor, α-particles will heat electrons, which will then heat ions, it would be preferable to operate in a regime

where the ions and electrons are more closely coupled. As the figure shows, some NBI heated high performance plasmas now fall outside the true hot ion regime and so are evolving in the right direction.

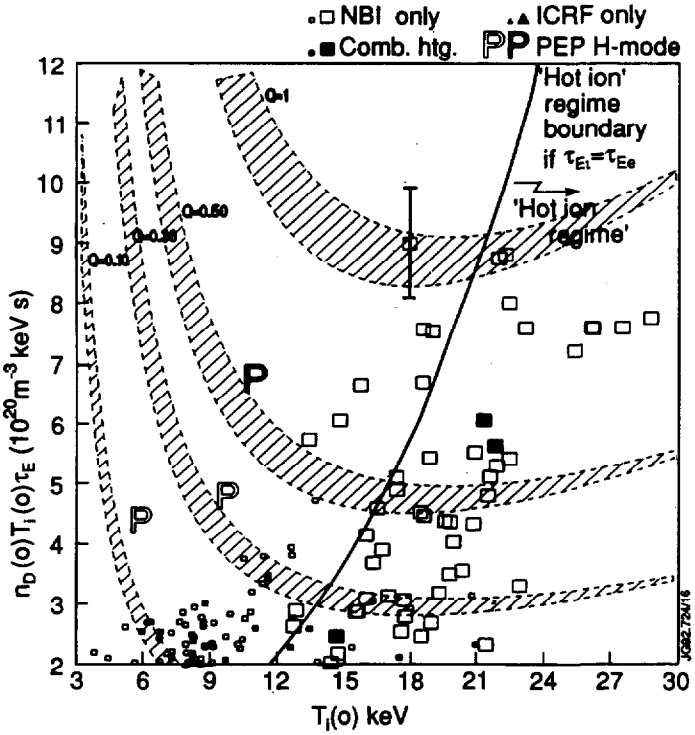

Fig. 8: Fusion performance of JET plasmas summarized in terms of the fusion triple product versus central ion temperature. The shaded regions correspond to the indicated values of Q for a 50:50 DT mixture. Points to the right of the line are in the 'hot ion' regime.

4. The Preliminary Tritium Experiment

The progressive improvement in the fusion performance of JET plasmas by 1991 suggested that the use of a deuterium/tritium mixture, even at low concentrations of tritium, would provide important information for the fusion programme as a whole and for the planning of JET's future programme in the lead up to the full DT experiment planned for 1996. Any such experiment would be severely constrained, however, by the continuing upgrades to JET which limit the acceptable activation of the torus and surrounding structure. Consequently a preliminary tritium experiment was undertaken with the following aims [1]:

- To demonstrate the technology related to tritium usage.
- To establish safe procedures for handling tritium in compliance with regulatory requirements.
- To provide data on the DT reactivity of JET plasmas for the calibration of transport codes which are used to extrapolate from DD to DT plasmas.

- To investigate the retention of tritium in the internal surfaces of the tokamak and to establish means for its removal.

- To produce over 1MW of DT fusion power.

The plasma scenario chosen for the experiment was a 3.1MA/2.8T hot ion H-mode discharge, such as that illustrated in Fig. 6, with the tritium being introduced into the plasma by 2 of the 16 neutral beam sources. This limited the tritium concentration of the plasma to ~10%, as required, and had the advantage of minimizing the quantity of tritium which had to be removed subsequently from the torus. The first successful demonstration of high power injection of tritium was, in itself, a major achievement of the experiment.

To limit the activation of the tokamak, only two high power pulses were attempted at maximum tritium concentration (11%). In addition, a sequence of pulses was performed at much lower concentration (1% tritium in the normal deuterium gas feed to two NBI sources). This permitted the final scenario to be optimized and also allowed specific experiments on tritium diffusion to be carried out. An overview of one of the two pulses which produced in excess of 1MW of fusion power is shown in Fig. 9. The general characteristics, including the termination of the high performance phase, are very similar to the hot ion discharges discussed previously, with the main difference being that the emission rate of 14.1MeV neutrons is more than an order of magnitude greater than that of the 2.4MeV neutrons produced in an equivalent pure deuterium plasma. At the peak fusion reaction rate, 6×10^{17}neutron/s were produced, equivalent to 1.7MW of fusion power, and the total fusion energy released was 2MJ.

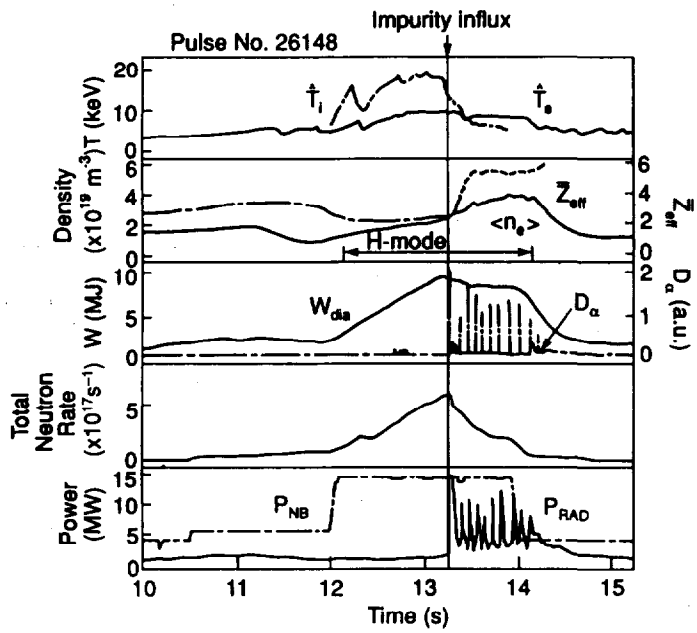

Fig. 9: Overview of one of the two pulses in which an 11% concentration of tritium was used, producing over 1MW of fusion power.

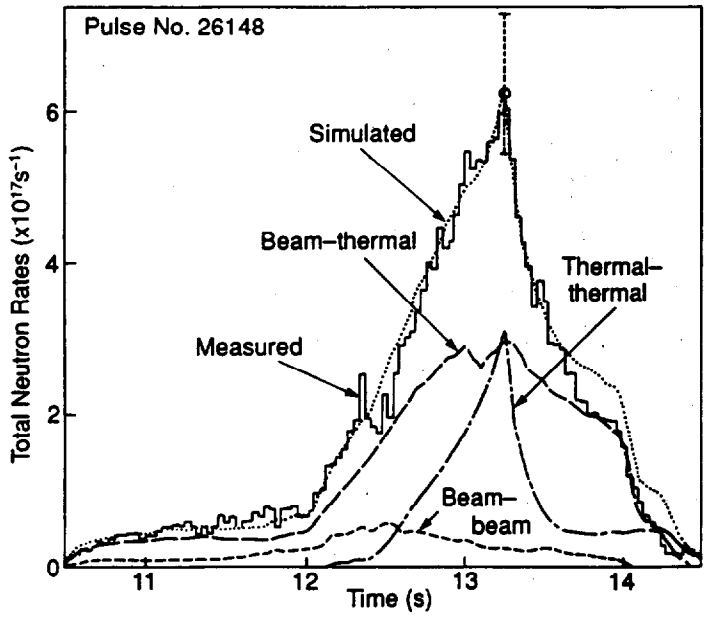

Fig. 10: Measured 14.1MeV neutron yield for a DT pulse compared with that calculated from measured plasma profiles. Approximately 50% of the neutron emission is from thermal reactions.

At the low tritium concentrations used in the PTE, the rate of α-particle production was expected to be too low to contribute significantly to the plasma heating. This was confirmed by subsequent analysis which showed that the α-particle power contributed less than 17% of the central electron heating power and less than 1% of the central ion heating power, too low to be resolved. Analysis of the neutron production for these plasmas (Fig. 10) showed that, at the peak of the fusion power production, approximately 50% of the neutrons were produced by thermonuclear reactions, with the remainder coming largely from reactions between beam ions and the thermal plasma. Less than 5% of the neutrons came from reactions between beam ions.

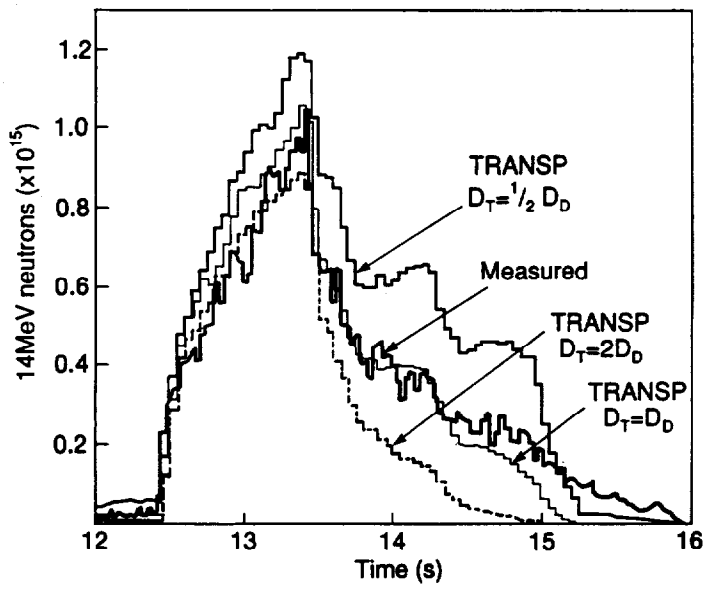

Fig. 11: Measured time evolution of 14.1MeV neutron emission for a pulse with a low tritium concentration compared with numerical simulations in which the indicated ratios of the tritium to deuterium diffusion coefficients, D_T/D_D, were used.

Further important information which was gleaned from pulses with tritium injection included a determination of the relative diffusion coefficients of deuterium and tritium [18]. This was obtained by analyzing plasmas with low concentrations of tritium, utilizing measurements of the spatial profiles of 14.1MeV neutron emission and of the decay of the neutron emission. As illustrated in Fig. 11, the results showed that good agreement between the calculated and measured decay rates of 14.1MeV neutrons could be obtained under the assumption that the diffusion coefficients of tritium and deuterium were equal. If the relative values were varied by a factor of 2 either way, there was clear disagreement with the experimental measurements.

In the course of the PTE, careful measurements were made of the tritium removed from the torus and the neutral beam lines. These showed that virtually all of the tritium introduced into these systems was recovered, within the 10% measurement errors. In fact, subsequent analysis of tiles removed from the torus and of outgassing of the neutral beam system suggested that more than 98% of the tritium used had been recovered. Thus, the overall aims of the experiment were successfully accomplished.

5. The New Phase of JET: The Pumped Divertor

In early 1992, JET began an extensive upgrade during which a Pumped Divertor [20] was installed. This, together with several other new facilities, is intended to inaugurate a new phase of the JET programme with two major aims:

- To demonstrate effective impurity control methods in conditions close to those of ITER.
- To investigate α-particle heating and confinement in an extensive DT experiment.

The capability of maintaining high power plasmas in quasi-steady-state conditions is a major feature of the new configuration. A poloidal cross-section of the upgraded tokamak, which will be capable of confining single null X-point plasmas at currents of up to 6MA, is illustrated in Fig. 12 and the main components of the Pumped Divertor are shown in Fig. 13. The principal features are:

- internal coils to produce an X-point equilibrium with a long connection length (5-10m) and to permit strike point sweeping to improve power handling;
- an improved target design and divertor geometry to optimize the distribution of exhaust power and to minimize impurity generation;
- a cryopump operating at liquid helium temperatures to pump neutral gas.

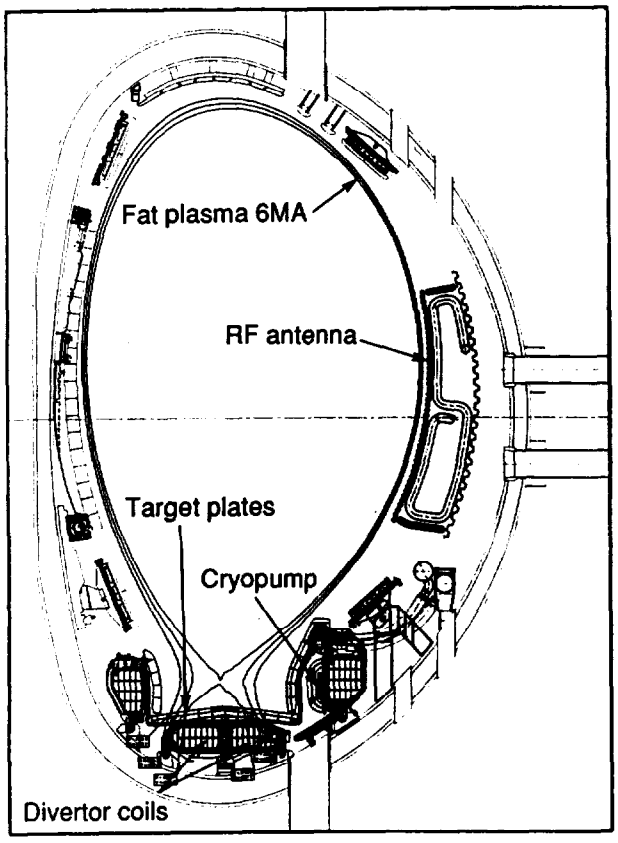

Fig. 12: poloidal cross-section of the upgraded JET tokamak showing the new features associated with the Pumped Divertor.

In addition to the Pumped Divertor, many of the tokamak subsystems have been extensively upgraded. This includes: improvements in all of the auxiliary heating systems; an improved fuelling system consisting of distributed gas and multiple pellet injection; internal saddle coils with 4.5MVA/10kHz power amplifiers for mhd stabilization experiments; and many new diagnostic systems, particularly for edge and divertor measurements.

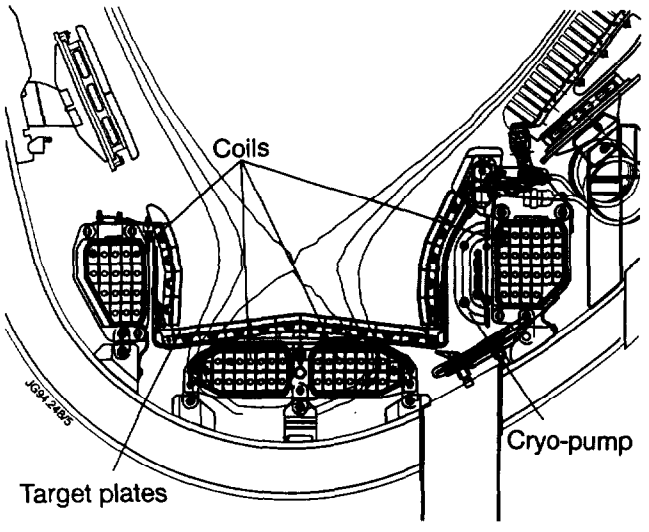

Fig. 13: The main components of the Pumped Divertor.

The first plasmas have now been achieved in the new configuration. X-point discharges at 2MA/2.7T with a current flat-top of up to 10s have been established. The experimental programme, which began in February 1994, is intended to address major issues, relating both to the bulk plasma and to the divertor, which must be resolved for ITER. In the former area, the physics of heating, confinement and mhd stability still hold many unknowns which make the extrapolation to ITER uncertain, while the key nature of the latter area has only been recognized relatively recently. There are, therefore, many problems, relating to the dissipation of exhaust power, the screening of impurities and the pumping of helium ash which must be resolved.

6. Summary

In its original incarnation JET has come within a factor of 6 of the plasmas parameters required for ignition, though only transiently. This performance has been exploited in the first tokamak experiments using a deuterium/tritium mixture, with the result that over 1MW of fusion power was produced. The PTE also allowed many aspects of tritium handling technology to be successfully demonstrated. Extensive investigations of the relative merits of carbon and beryllium as plasma facing materials have been performed. While carbon has better power handling capabilities, particularly at low to moderate densities, beryllium has allowed access to high density divertor regimes which may be more relevant for ITER.

The Pumped Divertor upgrade has equipped JET with an extensive set of facilities which will allow both physics and technology questions for ITER to be addressed. The future experimental programme will focus on the two main areas of divertor physics and the physics of DT plasmas. However, the flexibility and scale of the JET tokamak make it an ideal experiment for the investigation of the many detailed questions of stability and confinement which must be solved in the development of a fusion reactor.

Acknowledgements

The results presented in these lectures represent the product of the labours of my many colleagues in the JET Team, who, over many years, constructed the tokamak and its auxiliary systems, planned and performed the experiments, and analyzed the data.

References

[1] The JET Team, Nucl. Fusion **32** 187 (1992).
[2] M Chatelier, these Proceedings.
[3] P S Stangeby and G M McCracken, Nucl. Fusion 30 1225 (1990).

[4] The JET Team (presented by K J Dietz), Plasma Phys. and Contr. Fusion **32** 837 (1991).

[5] The JET Team (presented by P R Thomas), in *Plasma Physics and Controlled Fusion Research 1990* (Proc. 13th Int. Conf., Washington, 1990) Vol. 1, IAEA, Vienna (1991) 375.

[6] The JET Team (presented by G Janeschitz), in *Plasma Physics and Controlled Fusion Research 1992* (Proc. 14th Int. Conf., Würzburg, 1992) Vol. 1, IAEA, Vienna (1993) 329.

[7] M Ulrickson et al, J. Nucl. Mater. **176-177** 44 (1990).

[8] C G Lowry et al, J. Nucl. Mater. **196-198** 83 (1990).

[9] F Tenney and G Lewin, *Princeton Plasma Physics Laboratory Report MATT-1050* (1974).

[10] M L Watkins and PH Rebut, Proc. 19th Euro. Conf. on Contr. Fusion and Plasma Phys., Innsbruck, 1992, **2** 731.

[11] S Clement et al, ibid **2** 723.

[12] C D Challis et al, Nucl. Fusion **33** 1097 (1993).

[13] M Keilhacker et al, Phys Fluids B **2** 1291 (1990).

[14] D A Boyd et al, Nucl. Fusion **29** 593 (1989).

[15] B J D Tubbing et al, Nucl. Fusion **31** 839 (1991).

[16] D P Schissel et al, Nucl. Fusion **31** 73 (1991).

[17] H Weisen et al, Nucl. Fusion **31** 2247 (1991).

[18] B Balet et al, Nucl. Fusion **33** 1345 (1993).

[19] E Thompson et al, Phys. Fluids B **5** 2468 (1993).

[20] The JET Team (presented by P.-H. Rebut), in *Plasma Physics and Controlled Nuclear Fusion Research 1990* (Proc. 13th Int. Conf. Washington, 1990) Vol. 1, IAEA, Vienna (1991) 27.